

Effects of oxygen on the electron transport properties of carbon nanotubes: Ultraviolet desorption and thermally induced processes

Moonsub Shim,^{1,*} Ju Hee Back,¹ Taner Ozel,² and Kwan-Wook Kwon¹

¹*Department of Materials Science and Engineering, University of Illinois at Urbana-Champaign, Urbana, Illinois 61801, USA*

²*Department of Physics, University of Illinois at Urbana-Champaign, Urbana, Illinois 61801, USA*

(Received 15 December 2004; published 26 May 2005)

Highly sensitive electrical response of carbon nanotubes to UV exposure and thermal treatments are examined. Low intensity UV-induced conductivity change in individual single-walled carbon nanotube transistors is found to be mainly arising from oxygen desorption at the metal contacts rather than from nanotubes or possible amorphous side products. Choice of metal or thermal annealing (which changes the metal-nanotube contacts) eliminates or minimizes this low intensity UV response. However, a slow p-doping process is observed upon thermal annealing followed by equilibration in O₂ or air as suggested by changes in the near infrared spectra of nanotube films and in individual nanotube transport characteristics.

DOI: 10.1103/PhysRevB.71.205411

PACS number(s): 73.63.Fg, 72.80.Rj, 68.43.Tj, 61.46.+w

I. INTRODUCTION

In the ideal limit, a single-walled carbon nanotube (SWNT) can be considered as a seamless cylinder of a rolled up graphene sheet without surface trap/defect states and provides a model system to explore physical and chemical properties of one-dimensional materials.¹ Furthermore, many potentially useful properties such as exceptionally high carrier mobilities of $\sim 100\,000\text{ cm}^2(\text{Vs})^{-1}$,² long electron-acoustic phonon scattering mean free path on the order of a micron,³ the highest density-normalized elastic modulus,⁴ and near infrared photoluminescence^{5,6} have been reported. Applications in diverse areas from electronics^{7,8} to biomedical technologies⁹ have been considered. However, difficulties in determining intrinsic properties as opposed to behavior altered by external influences, often amplified by the fact that all atoms of SWNTs are at the surface, hinder many advances. For example, extremely oxygen-sensitive electron transport characteristics of SWNTs had initially been attributed to *p* doping by oxygen adsorption,^{10,11} possibly at defect sites, but later other factors such as oxygen adsorption at nanotube-metal contacts have been suggested to be important.¹² Covalently bound oxygen especially from purification and processing steps can result in drastically altered properties reminiscent of *p* doping which may be removed by thermal annealing under inert atmosphere.¹³ Here, we explore how oxygen affects electron transport characteristics of SWNTs by studying low intensity UV and thermal annealing induced changes.

Large conductance changes in both individual semiconducting SWNTs and SWNT “mats” upon irradiation of low intensity UV have recently been reported to arise from desorption of oxygen.¹⁴ It has further been shown that this large conductance change does *not* arise from changes in doping levels.¹⁵ Whether this UV-induced effect is an intrinsic response of SWNTs or an extrinsic factor related to, for example, metal contacts or amorphous residues has not yet been resolved. SWNT transistors with relatively high contact resistance often exhibit behavior that can be described as Schottky barrier transistors¹² whereas SWNTs with small contact resistance can be described much like conventional

field-effect transistors with diffuse transport or, in the case of relatively short channel lengths, as ballistic transistors.^{16,17} We show here that the conductance changes observed upon low intensity UV irradiation arise from oxygen desorption at the contacts when the contact metal has a large photodesorption cross sections. Different chemical vapor deposition (CVD) growth methods are used to exclude effects of amorphous side products. Different types of metal electrodes are used to examine the effects of contacts. Comparison between responses to UV exposure and thermal annealing is also made where differences suggest that slow doping effects from O₂ can arise.

II. EXPERIMENT

Transistors of SWNTs were fabricated using the patterned CVD method described previously.¹⁸ Two different growth conditions were employed. In both cases, catalyst islands were deposited on a heavily doped Si substrate with $\sim 400\text{ nm}$ thick thermal oxide patterned by deep UV using poly(methyl methacrylate) (PMMA) as resist. The standard CH₄ CVD growth technique was used in the first method.¹⁹ Briefly, Fe/alumina catalyst [15 mg Fe(NO₃)₃·9H₂O and 20 mg Al₂O₃ powder suspended in 20 ml methanol] was patterned on SiO₂/Si substrates by spin casting and liftoff then reduced under H₂/Ar flow. Growth was carried out at 900 °C with ultrahigh purity CH₄ and H₂ as the carbon feedstock and the dilution gas, respectively. In the second method, we adapted ethanol CVD procedure by Murakami *et al.*²⁰ into the patterned CVD process. The Co/Mo catalysts [0.1 wt % ((CH₃CO₂)₂Mo)₂ and 0.2 wt % (CH₃CO₂)₂Co·4H₂O in ethanol] were deposited onto a patterned SiO₂/Si substrate by spin casting. After PMMA liftoff and calcining in air at 400 °C for 5 min, CVD growth was carried out at 800 °C. Ethanol was introduced by bubbling Ar through a room temperature ethanol bath and the Ar flow rate was adjusted to maintain pressure at the inlet of ~ 3 torr during the growth period of 5 min.

Different metal sources used for electrical contacts were (1) $\sim 50\text{ nm}$ Ti (Ti-only), (2) ~ 10 to 20 nm Ti layer with 40

or 50 nm Au on top (thick-Ti/Au), (3) ~ 3 nm Ti adhesion layer with ~ 50 nm Au (thin-Ti/Au), and (4) ~ 30 nm Pd with ~ 20 nm Au capping layer (Pd contacted). In all four cases, metal contacts are evaporated on top of SWNTs with electrode separation of 2 or 4 μm .

Monochromatic light from a SPEX Fluoromax-3 spectrofluorometer with a 150 W ozone-free Xe arc lamp was collected with a quartz fiber optic and used as low intensity light source. In these cases, light intensities are < 2 mW cm^{-2} . For higher intensities, light from a 300 W ozone-free Xe arc lamp fitted with an IR filter and a bandpass filter centered at 3.65 eV (340 nm) with full width at half maximum (FWHM) = 0.93 eV (85 nm) was focused onto the samples. Neutral density filters were used to vary the intensity. The spot size was kept at ~ 1 cm diameter in both cases to maintain uniform intensity over the samples. Intensities were measured by precalibrated Si photodiode (Thermo Oriel). Temperature was monitored with a thermocouple placed directly on the SiO_2/Si substrates during UV exposures. The maximum temperature change was less than 1°C at the highest intensities (in all cases, UV intensities were ≤ 10 mW cm^{-2}) and heating effects from the light source were ruled out. Vacuum measurements were conducted at a base pressure of 10^{-7} to 10^{-6} torr.

Films or mats of SWNTs were obtained by spraying ethanol suspension of arc-discharge SWNTs purchased from Carboxex onto glass or sapphire substrates. To minimize any effects arising from processing, ethanol suspensions were made by sonicating as-received SWNTs in a low-power (70 W) sonicator for 5 min immediately prior to use. Near IR spectra were collected with Thermo Nicolet Nexus 670 FTIR equipped with thermoelectrically cooled InGaAs detector.

III. EFFECTS OF GROWTH CONDITIONS ON THE UV RESPONSE

In both individual SWNT transistors and mats of SWNTs, large decreases in conductance upon low intensity UV exposure have been observed and have been attributed to photo-desorption of oxygen.¹⁴ However, where desorption occurs and how it alters the conductivity remain unclear. We have previously shown by a combination of electron transport and optical measurements that the conductance changes in SWNTs upon UV irradiation do not arise from dopant removal and it is unlikely that low intensity UV exposure leads to desorption of covalently bound oxygen on possible defects on the sidewalls of the nanotubes.¹⁵ Other possible sites of desorption include the metal contacts, residues and sideproducts either from growth (e.g., amorphous carbon) or micro-fabrication processes, and substrate. We first examine effects of growth conditions on the response of SWNTs to UV exposure.

Utilizing hydrocarbons as the carbon source can often lead to unwanted side products, especially amorphous carbon. Although CH_4/H_2 CVD has been one of the best established methods for growing high quality SWNTs, small variations in the growth conditions can lead to significant amorphous carbon content. For example, small changes in

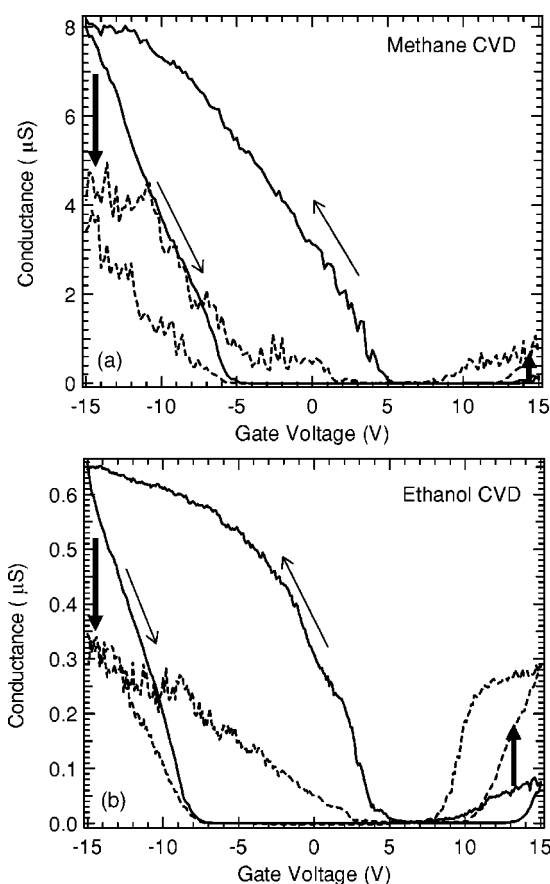


FIG. 1. The transfer characteristics of individual SWNT transistors before (solid curves) and after (dashed curves) 4 min exposure to 3.65 eV (340 nm) UV light with intensity ~ 3 mW cm^{-2} . Similar responses are observed for SWNT transistors fabricated using CH_4 CVD (a) and ethanol CVD (b). Drain-source bias is 100 mV in both cases.

the H_2 concentration have been shown to lead to mostly amorphous carbon, mostly SWNTs, or completely inactive regime where no products are formed.²¹ When ethanol is used as the carbon source for CVD synthesis, oxygen-based reactive species generated within the growth chamber presumably etch away amorphous carbon leading to high purity SWNTs without any additional processing.²⁰ Similar results have also been shown more recently with the addition of water vapor to hydrocarbon-based CVD synthesis.²² Transmission electron microscopy indicates that significant variations on the amount of amorphous carbon residues along the sidewalls can occur in CH_4/H_2 CVD synthesis whereas little or insignificant amorphous carbon coating is seen in ethanol CVD. By comparing the responses of SWNTs grown by CH_4/H_2 and ethanol-based growth, potential effects, if any, arising from amorphous side products that contribute to UV induced conductivity changes may be elucidated.

The responses of SWNTs grown by different CVD processes are compared in Fig. 1. Individual SWNT transistors fabricated using CH_4/H_2 and ethanol CVD are shown in Figs. 1(a) and 1(b), respectively. Both devices are exposed to 3.65 eV (340 nm) UV light with intensity ~ 3 mW cm^{-2} for 6 min under Ar. Other than the growth conditions, all other

conditions are the same for these two devices including the metal contacts which are thick-Ti/Au contacts. Both exhibit significant decrease in the p -channel conductance and simultaneous increase in n channel without noticeable threshold shift as previously reported.¹⁵ Forward (negative to positive) and reverse sweeps are shown here to ensure that possible threshold voltage shifts are not hidden by the hysteresis associated with individual SWNT transistors.^{23–26} Ethanol CVD grown SWNT in Fig. 1(b) exhibits $\sim 65\%$ p -channel decrease whereas SWNT grown by CH_4/H_2 CVD in Fig. 1(a) shows $\sim 50\%$ decrease. Longer exposure leads to slightly further decrease in the p channel for both cases. Since there are variations in the magnitude of conductance changes even within SWNTs grown with the same conditions, we cannot conclude that SWNTs by ethanol CVD, in general, exhibit larger response. However, SWNTs from both CVD processes show the same qualitative response to low intensity UV. We have also varied the CH_4/H_2 ratio by changing H_2 concentrations by nearly a factor of 2 where more amorphous carbon side-products may be expected²¹ but no qualitative differences in the responses to low intensity UV have been observed. These results suggest that direct or indirect effects arising from amorphous carbon side-products are *not* likely to be responsible for the observed UV response.

IV. ROLE OF METAL CONTACTS

In most nanoscale materials and molecules, electrical contacts to metal electrodes pose significant challenges and large contact resistances can often dominate the observed behavior. One of the controversial debates revolving around SWNT electron transport characteristics has been metal contacts to semiconducting SWNTs.^{12,17} One possible effect from metal contacts in the UV-induced conductivity changes in SWNTs may arise from variations in the metal work function brought on by oxygen desorption at the metal surface which may then change or create Schottky barriers. The work function of Ti is ~ 4.3 eV, which is smaller than expected work function of SWNTs (~ 4.5 – 5 eV for semiconducting SWNTs assuming the work function to be measured from midgap^{27,28}) and Schottky barriers may be expected. However, surface oxide formation and other molecular adsorption (e.g., hydrocarbons) are expected from ambient air and the work function may be significantly larger, resulting in small or insignificant Schottky barriers. On the other hand, the work functions of Au and Pd (between ~ 5.1 and 5.6 eV) are larger than those of SWNTs to begin with and Ohmic contacts have been shown to form with these two metals.^{16,17} Although a more complex situation is expected (e.g., due to possible tunnel barriers with different heights and widths near or at the contacts²⁹ and dependence on contact geometry¹²), for simplicity, we will refer to Ohmic p contacts when the metal Fermi level is pinned at or below the valence band edge of semiconducting SWNT and Schottky barrier contact when it lies above.

Figure 2 compares the transfer characteristics of SWNTs with different metal contacts. The insets are the corresponding I - V characteristics when the devices are turned on at gate

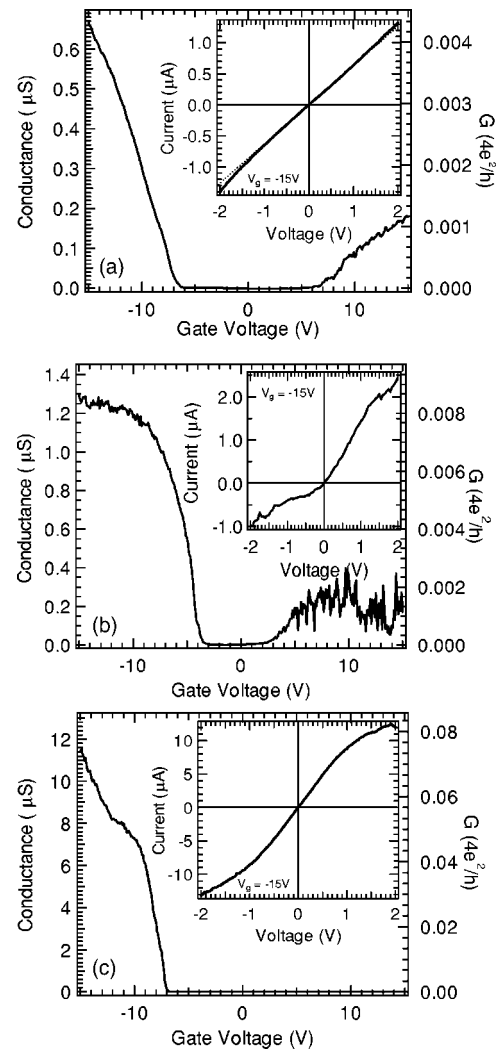


FIG. 2. The comparison of transport characteristics of SWNTs with different metal contacts. The transfer characteristics shown in (a) and (b) are for SWNTs contacted with >10 nm Ti with 50 nm Au capping layer (Ti-SWNT contacts). Pd-contacted SWNT is shown in (c). Titanium as contacts can lead to high on-state conductance with linear I - V characteristics (inset a) at large negative gate voltages but sometimes non-linear rectifying behavior is also seen (inset b). The I - V characteristic of Pd-contacted SWNT at the indicated gate voltage is shown in the inset of (c).

voltage, $V_g = -15$ V. Ti-contacted SWNTs can exhibit nearly linear I - V characteristics at large negative gate voltages [Fig. 2(a) inset], but sometimes nonlinear rectifying behavior [Fig. 2(b) inset] which may be associated with asymmetric tunnel junctions at the contacts²⁹ and/or Schottky barriers¹² is observed. Pd-contacted SWNTs with high on-state conductance show linear I - V characteristics at low voltages and begin to saturate at higher voltages suggesting MOSFET-like behavior [Fig. 2(c) inset]. If UV-induced conductivity changes are due to photodesorption of oxygen from metal electrodes altering or creating Schottky barriers at the contacts, different responses can be expected from the choice of metals that have different Fermi level pinning. When the photodesorption cross sections of metal contacts differ by orders of magnitude, even larger difference can be expected.

A. Ti contacts

Metal contacts with Ti-only and Ti adhesion layer significantly thicker than the diameter of SWNTs may both be considered to make Ti-SWNT contacts. Note that the edges of the Ti adhesion layer of Au electrodes where contacts to nanotubes occur are exposed to air in the current fabrication methods. Previous reports of UV-induced conductivity changes^{14,15} have also utilized such Ti contacts (with the Ti adhesion layer significantly thicker than the diameter of SWNTs with a Au capping layer). In these Ti-contacted SWNTs, large conductance changes due to UV-induced desorption of oxygen are consistently observed as shown in Figs. 1(a) and 1(b). When SWNTs are contacted with thin-Ti/Au electrodes (i.e. ~ 3 nm Ti adhesion layer, similar to or only slightly thicker than SWNT diameter), a very small or insignificant UV response is often observed, suggesting the importance of metal contacts on the observed UV-induced changes.

Figure 3(a) shows the I - V characteristics of Ti-only contacted SWNT before (thin line) and after (bold line) 11 min exposure to UV under Ar. Corresponding transfer characteristics are shown in the lower inset. Prior to UV exposure, relatively large p -channel on-state conductance and near linear I - V characteristics suggest, if present, small Schottky barriers for holes. Upon UV desorption, the expected large decreases in the p -channel transconductance and on-state current are accompanied by a nonlinear I - V curve, suggesting possible changes at the contacts.

Oxygen desorption in the form of CO_2 has been shown as the product of UV desorption from polycrystalline Ti films (with very thin oxide grown under O_2 at 100°C)³⁰ and similar desorption phenomenon at the oxide layer of Ti contacts may explain the behavior observed here. Figure 3(b) shows the decay of p -channel conductance (plotted in log scale as normalized conductance) upon UV exposure. If we assume that oxygen photodesorption occurs at the metal electrodes and that the metal work function changes linearly with the oxygen coverage $N=N_o \exp(-\sigma nt)$ over the exposure time t , then the change in the Schottky barrier height is proportional to

$$\Delta\phi \propto 1 - \frac{N}{N_o} = [1 - \exp(-\sigma nt)]. \quad (1)$$

Here, N_o is the initial oxygen coverage, σ is the photodesorption cross section, and n is the photon flux. Assuming thermionic emission to be the main contribution at room temperature, the conductance of the SWNT transistor, G , in response to photodesorption causing an increase in Schottky barrier height may then be estimated as

$$\ln\left(\frac{G}{G_o}\right) = -\frac{C}{kT}[1 - \exp(-\sigma nt)], \quad (2)$$

where G_o is the initial conductance, C is a constant related to the initial conditions (oxygen coverage and initial Schottky barrier height), and kT is the thermal energy. The solid curve in Fig. 3(b) is the least squares fit to Eq. (2). Using UV intensity $\sim 1.6 \text{ mW cm}^{-2}$ for 3.94 eV photons or photon flux of $\sim 2.5 \times 10^{15} \text{ cm}^{-2} \text{ s}^{-1}$ gives a photodesorption cross sec-

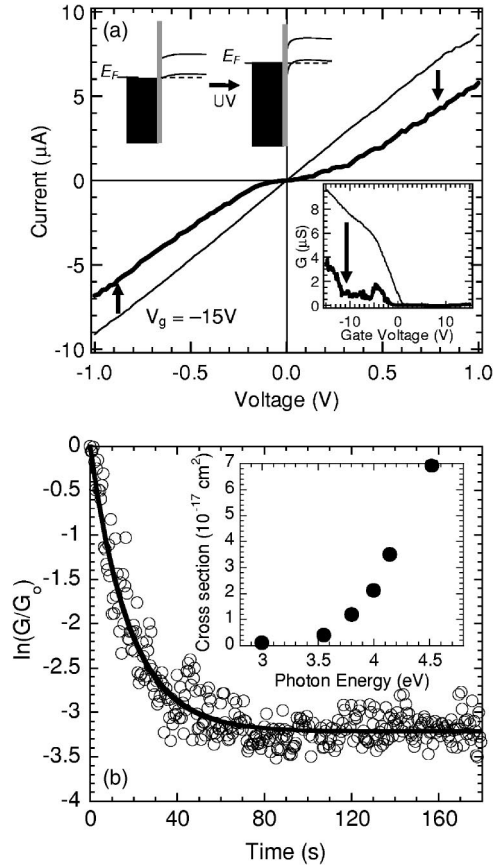


FIG. 3. The I - V curves before (thin curve) and after (bold curve) 11 min UV (photon energy = 3.65 eV) exposure under Ar for a Ti-only contacted SWNT transistor (a). The lower inset shows the corresponding transfer characteristics at $V_{DS} = 100$ mV. Note that the bold transfer curve in this inset is measured while the UV source is still on. The schematic of band alignment for p -channel operation before and after UV desorption of oxygen is shown in the upper inset. The change in the p -channel conductance, plotted as the natural log of the normalized conductance, due to exposure to UV (intensity $\sim 1.6 \text{ mW cm}^{-2}$ for 3.94 eV photons) is shown in (b). Only small voltages ($V_{DS} = 10$ mV and $V_g = 0$ V) were used to minimize any effects due to applied electrostatic potential. The solid curve is the least squares fit to Eq. (2) given in the text. The inset is the photon energy dependence of the photodesorption cross sections obtained from the least squares fits. Prior to measurements at each photon energy, the sample was heated in air at 100°C for 30 min to accelerate full recovery by enhancing surface oxidation (similar process as in Ref. 30).

tion of $\sim 2 \times 10^{-17} \text{ cm}^2$ from the fit. This value is consistent with reported photodesorption cross sections on the order of $\sim 10^{-17} \text{ cm}^2$ for metal oxides.³¹ Furthermore, photon energy dependence of the measured cross sections in the inset of Fig. 3(b) shows a threshold of ~ 3 eV (near the band gap of TiO_2) and a monotonic increase with photon energy. Similar dependence of oxygen photodesorption (measured as CO_2 signal) has been observed on Ti films with thin oxide layer.³⁰

These results indicate that the UV exposure leads to photodesorption of oxygen probably as CO_2 from the surface oxide layer of Ti contacts. Initially a relatively small or non-existent Schottky barrier (with possible tunnel barriers) be-

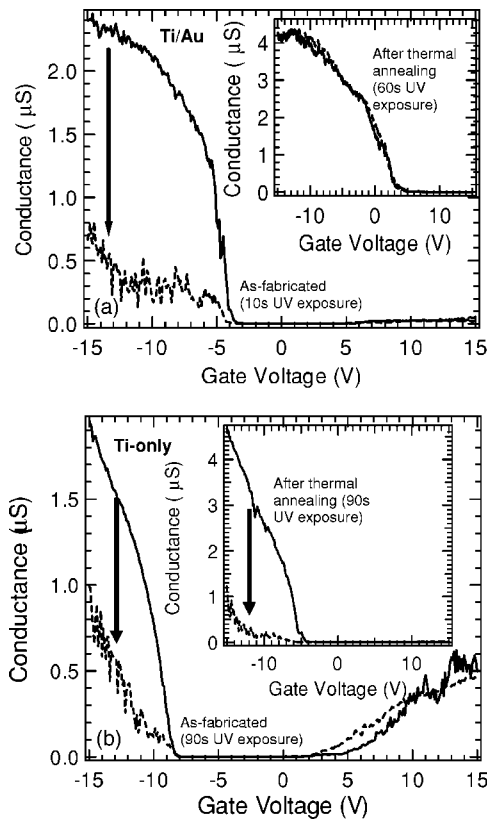


FIG. 4. The transfer characteristics showing the response of SWNT transistors to UV exposure before and after thermal annealing under Ar at 500 °C. Ti/Au contacted SWNT (a) exhibits large p -channel decay upon UV (photon energy=4.14 eV with intensity $\sim 1.8 \text{ mW cm}^{-2}$) irradiation before annealing but no longer responds after (inset). On the other hand, Ti-only contacted SWNT (b) exhibits large response to UV (photon energy=3.65 eV with intensity $\sim 3 \text{ mW cm}^{-2}$) before and after (inset) annealing.

comes larger as UV-induced oxygen desorption decreases the metal work function as illustrated in the upper inset of Fig. 3(a) for p -channel operation.

B. Au and Pd contacts

For a more direct confirmation that the UV-induced changes are due to desorption occurring at the metal contacts, we have also examined different metal electrodes. Initially, we annealed as-fabricated SWNT transistors under Ar to alter the contacts. Figure 4(a) shows the UV response of as-fabricated thick-Ti/Au contacted SWNT. A large response where nearly 80% decrease in p -channel on-state conductance occurs in 10 s of exposure is seen at shorter wavelength UV ($\lambda=300 \text{ nm}$, photon energy=4.14 eV with intensity $\sim 1.8 \text{ mW cm}^{-2}$). After annealing at 500 °C under Ar for 30 min and equilibrating in air for several hours, this device no longer exhibits UV-induced conductivity change [Fig. 4(a) inset] even at six times longer exposure time.

It had recently been shown that improved conductance in SWNT transistors upon thermal annealing may arise from the diffusion of Au atoms, resulting in Au-SWNT contacts rather than prior contact with the adhesion layer.¹⁷ If the

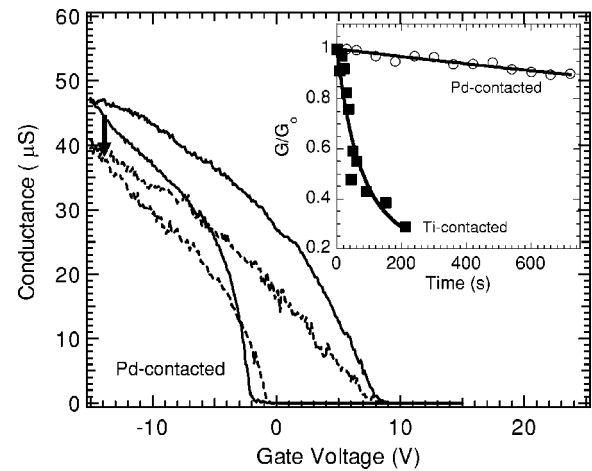


FIG. 5. The changes in the transfer characteristics of Pd-contacted SWNT to UV (photon energy=3.65 eV with intensity $\sim 10 \text{ mW cm}^{-2}$). The inset compares the p -channel conductance (average conductance between $V_g=-13$ and -15 V in the transconductance measurements) decay of Pd-contacted SWNT with Ti-contacted SWNT transistors at the same photon energy and intensity.

same process can be considered to occur in our annealing of Ti/Au contacted SWNTs, then the UV response observed prior to annealing is consistent with oxygen photodesorption from the surface oxide layer of Ti. Upon thermal annealing, which presumably results in direct Au-SWNT contact, UV desorption no longer becomes significant. This disappearance of UV response may be explained by considering that TiO_2 (i.e., oxide layer of Ti contacts) has large oxygen photodesorption cross sections and that noble metals such as Au do not. Changes in the contacts from Ti-SWNT to Au-SWNT upon thermal annealing may then be responsible for the large differences in the UV response. This mechanism is further supported by the fact that when Ti without Au capping layer is used as the contact metal, the UV response remains large even after thermal annealing at 500 °C under Ar as shown in Fig. 4(b) and its inset. However, caution must be taken as thermal annealing may induce effects other than the change in the nature of contact metal and is discussed further in the next section.

In order to avoid complications arising from other potential effects induced by thermal annealing, we have also examined SWNTs contacted with Pd where Ohmic contacts and ballistic transistors have been demonstrated without the need of thermal annealing to improve contacts.¹⁶ No significant effects are seen when Pd-contacted SWNT is exposed to low intensity UV. Only at our highest intensity of $\sim 10 \text{ mW cm}^{-2}$ at photon energy=3.65 eV (340 nm), a very small decrease in p channel begins to be noticeable when the SWNT transistor is exposed for an extended period of time (Fig. 5). The inset in Fig. 5 compares the p -channel conductance decay of Pd-contacted SWNT with Ti-contacted SWNT. Although the intensities and the photon energies are the same, Ti contacts lead to a very large response ($\sim 75\%$ decay in 200 s) whereas less than 10% decay occurs in 720 s for Pd contacts. These results are consistent with the expectation that Pd should have orders of magnitude smaller photodesorption cross sections than TiO_2 .^{32,33}

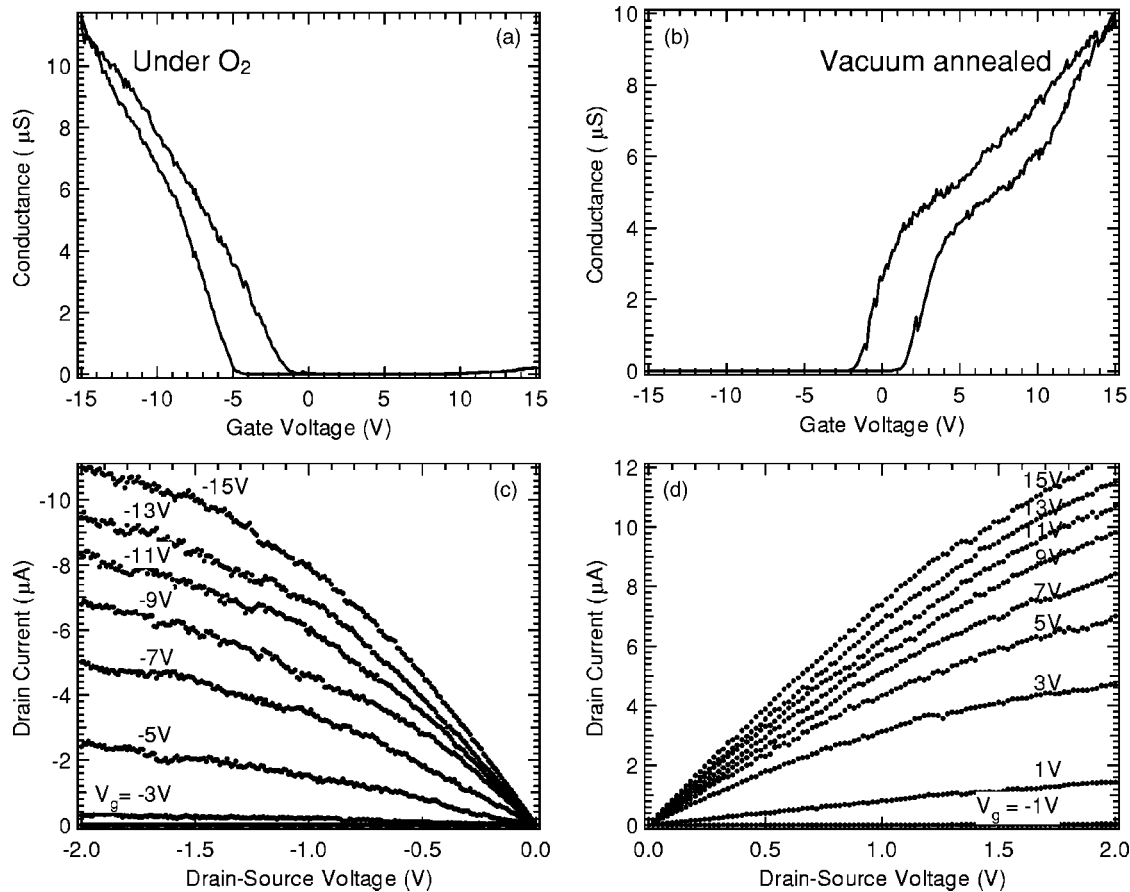


FIG. 6. The transfer characteristics of Pd-contacted SWNT under O_2 atmosphere (a) and in vacuum ($\sim 10^{-7}$ torr) after thermal annealing at $150^\circ C$ for 2 days (b). The drain-source voltage is 100 mV for both measurements. The p -channel output characteristics under O_2 and n -channel output under vacuum are shown in (c) and (d), respectively, with the corresponding gate voltages.

Combined with the fact that the smaller work function of Ti makes it easier to introduce Schottky barriers upon oxygen desorption, the differences in the UV responses of SWNT transistors with varying metal contacts observed here may be explained by photodesorption of oxygen at the metal electrodes. Low intensity UV-induced oxygen desorption creates Schottky barriers or, if present prior to exposure, increases the barrier heights for hole conduction. Oxygen is most likely desorbing from the oxide layer of Ti contacts as CO_2 in which case not only oxygen but also adsorbed hydrocarbons and other impurities are likely to play a role in the observed processes. This desorption would lead to decreased Schottky barrier for the electrons and can also explain the observed increase in the n -channel conduction upon UV irradiation for Ti-contacted SWNTs.

V. THERMAL ANNEALING AND DOPING EFFECTS

Thermal annealing of Ti/Au-contacted SWNT transistors leads not only to the disappearance of UV response, which is associated with changes in metal contacts, but also to other effects. The large threshold shift from -4 to $+3$ V observed in Fig. 4(a) suggests that O_2 exposure after thermal annealing leads to p doping. To sort out the effects arising at the contacts from other possible issues, we compare the transport

characteristics of Pd-contacted SWNT measured in O_2 to those measured under vacuum after thermal annealing. Figures 6(a) and 6(b) compare the transfer characteristics of p -type SWNT transistor measured in O_2 which is converted to n type under vacuum after annealing at relatively low temperatures ($150^\circ C$ for 2 days). Note that Fig. 6(a) is obtained after vacuum annealing followed by overnight equilibration under O_2 flow rather than measurements prior to annealing to provide a more direct comparison since other thermally induced effects such as diffusion of metal surface atoms may alter the contacts. Upon thermal annealing, surprisingly large n -channel conductance under vacuum [Fig. 6(b)], nearly as large as that of p channel measured under O_2 [Fig. 6(a)], is observed with completely suppressed p -channel conduction. The p -channel output characteristics in air are compared to those of n channel under vacuum in Figs. 6(c) and 6(d), respectively. Both show linear behavior in the low voltage regime with saturation at high voltages. While comparison with detailed modeling/computation will be necessary to verify exact transport mechanism and the influence of contacts, these high performance characteristics suggest Ohmic contacts with possibly small tunnel barriers [e.g., as illustrated in Fig. 3(b) inset left for p channel] with diffuse transport (due to relatively long channel length of $2 \mu m$) for both p and n channels.

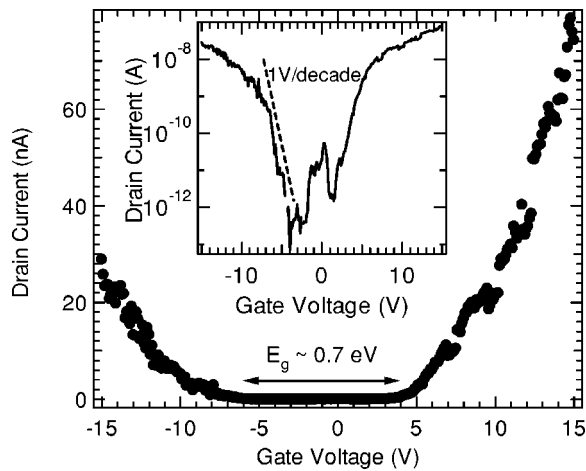


FIG. 7. The transfer characteristics of the same device as shown in Fig. 6 but prior to complete equilibration under O_2 . Both the p channel at negative gate voltages and the n channel at positive gate voltages are observed. The inset is the same curve plotted in log scale. The dashed line corresponds to subthreshold swing of 1 V per decade.

If Ohmic contacts to (or very small Schottky barriers for) n channel are achieved only by means of metal work function change from oxygen removal, thermal desorption of oxygen from the electrodes has to induce work function change similar to or larger than the band gap of the SWNT. Figure 7 shows the transfer characteristic of Pd-contacted SWNT (same device as in Fig. 6) measured under O_2 atmosphere prior to complete equilibration where both p - and n -channel conduction can be observed. The inset shows the same plot in log scale with subthreshold swing of ~ 1 V/decade (dotted line). This subthreshold swing corresponds to a gate efficiency parameter $\alpha \sim 0.06$ and the band gap can be estimated as $E_g = \alpha \Delta V_g$. With $\Delta V_g \sim 12$ V from Fig. 7, the band gap of this SWNT is ~ 0.7 eV. The estimated value of the band gap is consistent with expected value of 0.6 eV for a ~ 1.5 nm diameter SWNT (measured by AFM). At the temperature range of interest ($T \geq 300$ K), atomic oxygen (O) and not molecular oxygen (O_2) is expected on Pd surfaces.³² The maximum work function change due to O on Pd is 610 mV.³⁴ On certain faces, it is much smaller as in Pd (100) where a maximum work function change of 180 mV has been reported.³⁴ Furthermore, desorption of O from Pd is not expected to start until about 400 °C.³⁴ At our relatively low temperature annealing (150 °C), it is highly unlikely that O thermal desorption from Pd contacts can decrease metal work function by 600 mV or more. However, adsorbed hydrocarbons and other impurities may cause deviations and Cui *et al.* have shown that the contact potential difference between SWNT and polycrystalline Au changes almost 300 mV from ultra-high vacuum to air.³⁵ Even this relatively large value of 300 mV will result in ~ 400 mV Schottky barrier for electron conduction (assuming we begin with no Schottky barrier for the hole). This value is ~ 16 times the thermal energy at room temperature and therefore variations only due to metal work function change cannot account for the as large n -channel conductance observed in vacuum as p channel in

O_2 . Even if we consider Schottky barriers to exist, since the on-state conductance is nearly the same for both p and n channel, the barrier heights should be similar. This would lead to a minimum of ~ 200 mV Schottky barriers for both holes in Fig. 6(a) and electrons in Fig. 6(b). As a simple estimate for the conductance of a SWNT with a Schottky barrier of this magnitude, we can consider the maximum conductance in the SWNT transistor to be $\sim 4e^2/h \times \exp(-\phi/kT)$. Here, quantum conductance $4e^2/h$ is the maximum conductance expected for SWNTs in the ideal limit and the exponential term assumes thermionic emission over the Schottky barrier ϕ with thermal energy kT . Omitting the tunneling contribution for simplicity, then the estimate of the maximum conductance at room temperature for a Schottky barrier of 200 mV is $\sim 0.05 \mu S$ or $\sim 3 \times 10^{-4} (4e^2/h)$. This value is 200 times smaller than the n -channel on-state conductance observed in Fig. 6(b). Considering the relatively long channel length of $2 \mu m$ where electron-phonon scattering will significantly reduce overall conductance, the discrepancy becomes even larger. While this is an admittedly oversimplified picture and the effects arising from changes in or creation of Schottky barriers at the contacts may be important, orders of magnitude discrepancy suggests that another mechanism is more predominant here.

Possible doping effects of oxygen should also be considered. In Fig. 6(a), the p -channel threshold voltages are -5 and -1 V for forward and reverse sweeps, respectively. The thresholds for n -channel in Fig. 6(b) are -2 and $+1$ V, for forward and reverse sweeps. While hysteresis makes it difficult to determine absolute threshold voltages, the maximum difference between p -channel threshold and n -channel threshold should be about 6 V. This value is only 1/2 of the band gap ($\Delta V_g \sim 12$ V), suggesting a significant threshold shift and therefore doping changes upon O_2 exposure. Doping level changes in SWNTs may also alter the nature of SWNT-metal contacts, leading to observed behavior where n -channel conductance under vacuum is as large as that of p -channel under O_2 .

In most cases, larger threshold shifts are observed when SWNTs transistors are annealed at higher temperatures followed by air equilibration. Figure 8 shows the changes in the transfer characteristics of a thick-Ti/Au-contacted SWNT transistor before and after thermal annealing under Ar at 500 °C followed by equilibration in air for several hours. The large increase in on-state conductance at negative gate voltages is likely due to the change in metal contact from Ti-SWNT to Au-SWNT as discussed in the previous section. There is also a large shift in the threshold voltage indicative of doping level change. Although hysteresis, which has been attributed to occur from charge trapping in the substrate, prevents quantification of doping level changes, the forward and the reverse sweeps shown for both curves in Fig. 8 indicate that this threshold shift is larger than the width of the hysteresis and therefore p doping may be occurring. SWNTs with Ti-only contacts also show similar increase in on-state conductance and threshold shift upon thermal annealing [Fig. 4(b)]. The large increase in on-site conductance in this case where there is no Au may be due to better adsorption (e.g., better wetting) of Ti on SWNT upon annealing. More importantly, both Ti-only and Ti-Au-contacted SWNTs show posi-

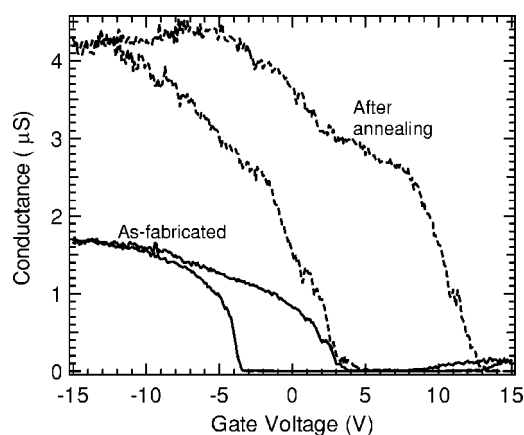


FIG. 8. The transfer characteristics of thick-Ti/Au-contacted SWNT before (solid line) and after thermal annealing under Ar at 500 °C (dashed line). Both forward and reverse sweeps are plotted to show that the threshold shift after thermal annealing followed by equilibration in air is larger than the hysteresis.

tive threshold shift significantly larger than the hysteresis.

Doping due to O₂ exposure is further confirmed by changes in the near IR absorption spectra of SWNT mats. An absorption bleach in the semiconducting SWNTs' band edge transitions in the near IR is expected upon injection of charge carriers. Figure 9 shows the near IR absorption spectra of SWNT mats under vacuum after thermal annealing at 400 °C for 3 h at $\sim 10^{-6}$ torr (solid curve) and after equilibrating in air for 4 days (dashed curve). Nearly complete bleach of the band edge transition at ~ 0.68 eV is observed upon air exposure. A direct comparison is difficult to make, especially since isolated individual SWNTs may be significantly influenced by substrates and SWNT mats may contain amorphous carbon and catalyst residues. However, this large absorption bleach is consistent with the apparent threshold shift observed in individual SWNT transistors indicating effects associated with doping.

We finally note that the time it takes to observe significant threshold shift comparable to or larger than the magnitude of the hysteresis varies from sample to sample (a few minutes for some but usually days to weeks for most). Variations in reoxidation times of SWNTs have been recently reported where peroxides have been suggested to form from reaction between singlet oxygen and SWNT sidewalls.³⁶ Here, we anticipate even larger variations since individual SWNTs rather than ensemble are examined. However, large positive threshold shift in individual SWNT transistors and band edge absorption bleach in the SWNT mats strongly suggest the importance of doping effects of ambient O₂.

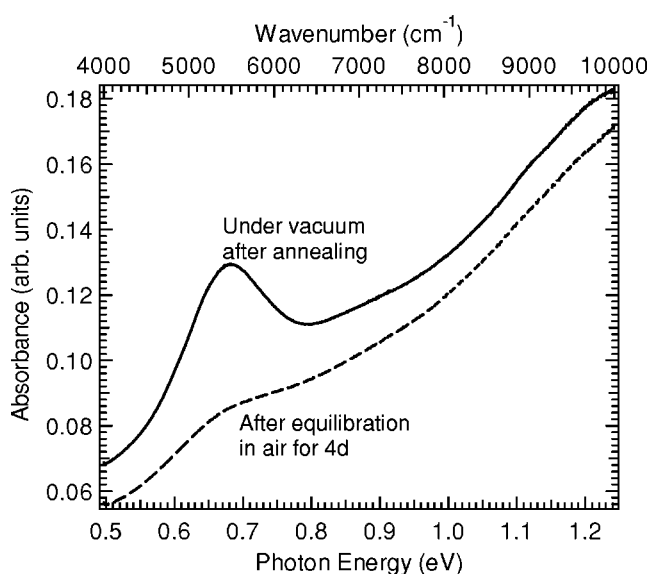


FIG. 9. The near IR absorption spectra of SWNT mats after thermal annealing under vacuum at 400 °C for 3 h. The solid curve is measured under vacuum and the dashed curve is measured in air after equilibrating for 4 days.

VI. CONCLUSIONS

Photodesorption and thermal annealing studies carried out here indicate that ambient O₂ can have important impact both on the SWNT-metal contacts as well as directly on SWNTs. We have shown that low intensity UV-induced conductance changes observed in SWNT transistors arise mainly from oxygen desorption at the oxide layer of Ti contacts increasing or creating Schottky barriers for hole transport. By choosing Pd or Au as contact metals, little or no UV-induced conductivity change is observed. Orders of magnitude smaller photodesorption cross sections in Pd and Au than in the oxide layer of Ti and the fact that former two metals are likely to form non-Schottky contacts can account for these observations. However, changes in the transport and near IR absorption properties upon thermal annealing and subsequent exposure to O₂ lead to variations consistent with doping effects of O₂ on SWNTs rather than behavior dominated by contacts. Further studies will be necessary to elucidate the oxidation mechanism.

ACKNOWLEDGMENTS

This work was supported by NSF Grant No. DMR-0348585 and ACS PRF. Atomic force microscopy and transmission electron microscopy of the samples were carried out in the Center for Microanalysis of Materials, University of Illinois, which is partially supported by the U.S. Department of Energy under Grant No. DEFG02-91-ER45439.

*Corresponding author. Email address: mshim@uiuc.edu

- ¹Carbon Nanotubes: Synthesis, Structure, Properties and Applications, edited by M. Dresselhaus, G. Dresselhaus, and Ph. Avouris (Springer, Berlin, 2001).
- ²M. S. Fuhrer, B. M. Kim, T. Durkop, and T. Brintlinger, Nano Lett. **2**, 755 (2002).
- ³J.-Y. Park, S. Rosenblatt, Y. Yaish, V. Sazonova, H. Ustunel, S. Braig, T. A. Arias, P. W. Brouwer, and P. L. McEuen, SAE Tech. Pap. Ser. **4**, 517 (2004).
- ⁴R. H. Baughman, A. A. Zakhidov, and W. A. de Heer, Science **297**, 787 (1998).
- ⁵M. J. O'Connell, S. M. Bachilo, C. B. Huffman, V. C. Moore, M. S. Strano, E. H. Haroz, K. L. Rialon, P. J. Boul, W. H. Noon, C. Kittrell, J. Ma, R. H. Hauge, R. B. Weisman, and R. E. Smalley, Science **297**, 593 (2002).
- ⁶A. Hartschuh, H. N. Pedrosa, L. Novotny, and T. D. Krauss, Science **305**, 1354 (2003).
- ⁷A. Bochtold, P. Hadley, T. Nakanishi, and C. Dekker, Science **294**, 1317 (2001).
- ⁸C. Zhou, J. Kong, E. Yenilmez, and H. Dai, Science **290**, 1552 (2000).
- ⁹R. J. Chen, S. Bangsaruntip, K. A. Drouvalakis, N. Wong Shi Kam, M. Shim, Y. Li, W. Kim, P. J. Utz, and H. Dai, Proc. Natl. Acad. Sci. U.S.A. **100**, 4984 (2003).
- ¹⁰P. G. Collins, K. Bradley, M. Ishigami, and A. Zettl, Science **287**, 1801 (2001).
- ¹¹G. U. Sumanasekera, C. Adu, S. Fang, and P. C. Eklund, Phys. Rev. Lett. **85**, 1096 (2000).
- ¹²S. Heinze, J. Tersoff, R. Martel, V. Derycke, J. Appenzeller, and Ph. Avouris, Phys. Rev. Lett. **89**, 106801 (2002).
- ¹³A. Kuznetsova, I. Popova, J. T. Yates, M. J. Bronikowski, C. B. Huffman, J. Liu, R. E. Smalley, H. H. Hwu, and J. G. Chen, J. Am. Chem. Soc. **123**, 10699 (2001).
- ¹⁴R. J. Chen, N. R. Franklin, J. Kong, J. Cao, T. W. Tomblor, Y. Zhang, and H. Dai, Appl. Phys. Lett. **79**, 2258 (2001).
- ¹⁵M. Shim and G. P. Siddons, Appl. Phys. Lett. **83**, 3564 (2003).
- ¹⁶A. Javey, J. Guo, Q. Wang, M. Lundstrom, and H. Dai, Nature (London) **424**, 654 (2003).
- ¹⁷Y. Yaish, J.-Y. Park, S. Rosenblatt, V. Sazonova, M. Brink, and P. L. McEuen, Phys. Rev. Lett. **92**, 046401 (2003).
- ¹⁸H. T. Soh, C. F. Quate, A. F. Morpurgo, C. M. Marcus, J. Kong, and H. Dai, Appl. Phys. Lett. **75**, 627 (1999).
- ¹⁹J. Kong, H. T. Soh, A. M. Cassell, C. F. Quate, and H. Dai, Nature (London) **395**, 878 (1998).
- ²⁰Y. Murakami, S. Chiashi, Y. Miyauchi, M. H. Hu, M. Ogura, T. Okubo, and S. Maruyama, Chem. Phys. Lett. **385**, 298 (2004).
- ²¹N. R. Franklin, Y. Li, R. J. Chen, A. Javey, and H. Dai, Appl. Phys. Lett. **79**, 4571 (2001).
- ²²K. Hata, D. N. Futaba, K. Mizuno, T. Namai, M. Yumura, and S. Iijima, Science **306**, 1362 (2004).
- ²³M. S. Fuhrer, B. M. Kim, T. Durkop, and T. Brintlinger, SAE Tech. Pap. Ser. **2**, 755 (2002).
- ²⁴M. Radosevljevi, M. Freitag, K. V. Thadani, and A. T. Johnson, Nano Lett. **2**, 761 (2002).
- ²⁵J. B. Cui, R. Sordan, M. Burghard, and K. Kern, Appl. Phys. Lett. **81**, 3260 (2002).
- ²⁶W. Kim, A. Javey, O. Vermesh, Q. Wang, Y. Li, and H. Dai, Nano Lett. **3**, 193 (2003).
- ²⁷S. Suzuki, Y. Watanabe, Y. Homma, S. Fukuba, S. Heun, and A. Locatelli, Appl. Phys. Lett. **85**, 127 (2004).
- ²⁸J. Zhao, J. Han, and J. P. Lu, Phys. Rev. B **65**, 193401 (2002).
- ²⁹J.-Y. Park and P. L. McEuen, Appl. Phys. Lett. **79**, 1363 (2001).
- ³⁰N. van Hieu and D. Lichtman, Surf. Sci. **103**, 535 (1981).
- ³¹Y. Shapira, R. B. McQuistan, and D. Lichtman, Phys. Rev. B **15**, 2163 (1977).
- ³²L. Hanley, X. Guo, and J. T. Yates, Jr., J. Chem. Phys. **91**, 7220 (1989).
- ³³G. Lu, A. Linsebigler, and J. T. Yates, Jr., J. Chem. Phys. **102**, 4657 (1995).
- ³⁴G. Ertl and J. Koch, in *Adsorption-Desorption Phenomena*, edited by F. Ricca (Academic, New York, 1972).
- ³⁵X. Ciu, M. Freitag, R. Martel, L. E. Brus, and Ph. Avouris, Nano Lett. **3**, 783 (2003).
- ³⁶G. Dukovic, B. E. White, Z. Zhou, F. Wang, S. Jockusch, M. L. Steigerwald, T. F. Heinz, R. A. Friesner, N. J. Turro, and L. E. Brus, J. Am. Chem. Soc. **126**, 15269 (2004).